Obtaining Local-Tie Vectors From Short-Baseline Interferometry Between Legacy S/X and VGOS Telescopes at Ny-Ålesund

Citation for the original published paper (version of record):
Handirk, R., Varenius, E., Nilsson, T. et al (2026). Obtaining Local-Tie Vectors From Short-Baseline Interferometry Between Legacy S/X and VGOS
Telescopes at Ny-Ålesund. Radio Science, 61(9): n/a-n/a. http://dx.doi.org/10.1029/2025RS008586

ADVANCING EARTH AND SPACE SCIENCES

Radio Science

RESEARCH ARTICLE
10.1029/2025RS008586

Obtaining Local-Tie Vectors From Short-Baseline Interferometry Between Legacy S/X and VGOS Telescopes at Ny-Ålesund

Rebekka Handirk[1], Eskil Varenius[1], Tobias Nilsson[1,2], Karine Le Bail[1], Rubén Bolaño González[3], Susana Garcia-Espada[3], Axel Meldahl[3], Thomas Gasmoe[3], Silje Agnes Grøslie Wennesland[3], Oddvar Bråvold Tangen[3], and Halfdan Pascal Kierulf[3]

[1]Onsala Space Observatory, Department of Physics and Astronomy, Chalmers University of Technology, Onsala, Sweden, [2]Lantmäteriet – The Swedish Mapping, Cadastral, and Land Registration Authority, Gävle, Sweden, [3]Norwegian Mapping Authority, Geodetic Earth Observatory, Ny-Ålesund, Norway

Key Points:

- The outcome of the NYTIE project are the local tie vectors between the legacy and the new generation VGOS telescopes at Ny-Ålesund
- We recommend observatories with several radio telescopes to conduct dedicated VLBI local tie experiments
- The results of this campaign will be an essential input for calculating the next International Terrestrial Reference Frame

Correspondence to:

R. Handirk,
rebekka.handirk@chalmers.se

Citation:

Handirk, R., Varenius, E., Nilsson, T., Le Bail, K., Bolaño González, R., Garcia-Espada, S., et al. (2026). Obtaining local-tie vectors from short-baseline interferometry between legacy S/X and VGOS telescopes at Ny-Ålesund. *Radio Science*, *61*, e2025RS008586. https://doi.org/10.1029/2025RS008586

Received 17 DEC 2025
Accepted 6 AUG 2026

Author Contributions:

Conceptualization: Eskil Varenius, Susana Garcia-Espada
Data curation: Rebekka Handirk, Eskil Varenius, Tobias Nilsson, Karine Le Bail
Formal analysis: Rebekka Handirk, Eskil Varenius, Tobias Nilsson
Investigation: Rebekka Handirk, Eskil Varenius, Tobias Nilsson, Karine Le Bail
Methodology: Rebekka Handirk, Eskil Varenius
Resources: Rubén Bolaño González, Susana Garcia-Espada, Axel Meldahl, Thomas Gasmoe, Silje Agnes Grøslie Wennesland
Software: Rebekka Handirk, Tobias Nilsson
Supervision: Eskil Varenius, Tobias Nilsson, Karine Le Bail

Abstract With the ongoing transition for geodetic Very Long Baseline Interferometry (VLBI) from the use of legacy S/X telescopes to the VLBI Global Observing System (VGOS), it is necessary to connect the new VGOS network to the existing legacy S/X telescopes. One way to do this is through specially designed short-baseline interferometry sessions with the aim to obtain local-tie vectors between these telescope generations at observatories that host both legacy S/X and new generation VGOS telescopes. The dismantling of the legacy S/X telescope NYALES20 at the Ny-Ålesund Geodetic Earth Observatory in August 2023 was preceded by around one and a half years of short-baseline interferometric measurements, referred to as NYTIE, to the new VGOS telescopes NYALE13S and NYALE13N. The results of these measurements are used to connect the old and new networks at this observatory. We present both group and phase delay results of this dedicated measurement campaign. We also analyze the same baselines with data that can be obtained from regular IVS-R1 and IVS-R4 sessions. We find a significant discrepancy between group and phase delay positions in the vertical component. Sensitivity tests attribute this discrepancy to session-dependent differential troposphere effects rather than to telescope deformation modeling. Both group and phase delay results are consistent with a classical geodetic survey using total station and GNSS once the formal uncertainties are rescaled to reflect the observed session-to-session scatter and a residual modeling systematic of 7 mm is taken into account.

Plain Language Summary Very Long Baseline Interferometry (VLBI) is a global network of radio telescopes that precisely measures the Earth's orientation and creates the most stable map of the planet. This field is undergoing a major upgrade, transitioning from an older generation of telescopes to a new generation called VLBI Global Observing System (VGOS). To maintain a continuous and accurate global map, it is essential that the historical data aligns perfectly with the new VGOS data. A critical measurement campaign was conducted at the Ny-Ålesund Observatory, where both old and new telescopes were operating side-by-side before the older one was decommissioned. Instead of relying on traditional ground survey tools, the highly accurate VLBI technique itself was used to measure the distance between the three instruments. This direct method avoids introducing external measurement errors. The central achievement of this research is the successful acquisition of these precise local-tie measurements. This data is immediately available to be included as an essential constraint when calculating the next International Terrestrial Reference Frame (ITRF), a realisation of the Earth's official global coordinate system. By using these constraints, the overall accuracy and stability of the ITRF, which underpins all modern navigation and climate science, is significantly strengthened.

1. Introduction

Very Long Baseline Interferometry (VLBI) is a radio-astronomical technique used both in astronomy and in geodesy (Nothnagel, 2025; Sovers et al., 1998). Geodetic VLBI is one of the four space geodetic techniques used for the determination of Earth Orientation Parameters (EOP) and the establishment of reference frames. However, it is the only technique that can deliver a connection between the celestial and terrestrial frames. VLBI is also used to obtain the relative distances between the participating telescopes.

Between October 1994 and August 2023, the Geodetic Earth Observatory Ny-Ålesund (GEON) (Garcia-Espada et al., 2023) participated in VLBI experiments with the legacy S (2 GHz) and X (8 GHz) telescope NYALES20

Validation: Rebekka Handirk, Eskil Varenius, Tobias Nilsson, Karine Le Bail, Oddvar Bråvold Tangen, Halfdan Pascal Kierulf
Visualization: Rebekka Handirk
Writing – original draft: Rebekka Handirk
Writing – review & editing: Rebekka Handirk, Eskil Varenius, Tobias Nilsson, Karine Le Bail, Susana Garcia-Espada, Halfdan Pascal Kierulf

(Ny). Since 2020 resp. 2022 also the VLBI Global Observing System (VGOS) telescopes NYALE13S (Ns) and NYALE13N (Nn) are officially observing for the International VLBI Service for Geodesy and Astrometry (IVS) (Nothnagel et al., 2017). The shift from legacy S/X to VGOS at observatories worldwide demands a careful validation of the local ties between the legacy and VGOS instruments to ensure that the site coordinates remain consistent across both networks. Moreover, the simultaneous operation of both telescope generations at GEON provided a vital opportunity to establish a direct link between the legacy and the new VGOS reference frame realizations.

Since 2018, the IVS schedules a few experiments each year with networks that contain both types of telescopes (see McCallum et al., 2022). However, up until July 2023, Nn had not been included in any of such mixed-generation experiments despite being operational since November 2022. Instead, it was solely involved in sessions with the VGOS network. As detailed in Section 2, Ns was operated in S/X configuration during the period covered by this study (2022–2023), and participated exclusively in experiments with other legacy telescopes. This created a scenario where two instruments with legacy equipment (Ny and Ns) coexisted with a dedicated VGOS instrument (Nn), but remained disconnected in terms of reference frame realisation.

By keeping the S/X and VGOS networks separate, two different realizations of the Terrestrial Reference System (TRS) are created. In this particular case, this means that the link between the two TRS realizations is weak at GEON. However, given its unique high-latitude geographical location, GEON is critical for maximizing the overall network volume, a factor which significantly impacts the quality of estimated EOP from geodetic VLBI (Malkin, 2009). Therefore, establishing a strong local link at this site is of great importance.

The opportunity to establish this link at GEON was time-constrained by the imminent dismantling of the legacy telescope Ny in August 2023. In order to enable the continuity of the long-term legacy record and to improve the integration with the new VGOS generation, we exploited the final operational overlap of Ny with Ns and Nn to conduct a series of dedicated short-baseline experiments, referred to as NYTIE. These experiments, carried out between March 2022 and August 2023, aimed to obtain the local ties between Ny and the new telescopes Ns and Nn for the next International Terrestrial Reference Frame (ITRF) (Altamimi et al., 2016). This paper presents the results of the analysis of short-baseline interferometry experiments conducted at Ny-Ålesund before the legacy telescope NYALES20 was dismantled and stopped operations in August 2023. The results could be included in the calculations of the next ITRF.

Dedicated short-baseline experiments have been successfully conducted at the Onsala Space Observatory (OSO) by Varenius et al. (2021) and Handirk et al. (2023), as well as at the Kokee Park Geophysical Observatory by Niell et al. (2021). The results of these have already contributed to the computation of the ITRS 2020 realization of DGFI-TUM (DTRF2020 by Seitz et al., 2026).

However, it is not sufficient to conduct these local-tie measurements at just one station. They need to be undertaken at each observatory that hosts at least one telescope of both the legacy and the new generation systems. Contrary to the classic approach of engineering geodetic measurements with a total station and the use of Global Navigation Satellite Systems (GNSS) for local co-location surveys, we use the telescopes themselves to obtain their relative positions by using the VLBI technique on the short baselines.

Instead of developing dedicated experiments, one might also try utilizing data obtained from regular IVS experiments with tag-along constellations. A tag-along session is one where an otherwise unscheduled station observes the same sources (when visible) as another station and/or the rest of the network, but its presence has no influence on the source selection or schedule. Xu et al. (2023) used such data obtained in regular experiments scheduled by the IVS which included co-located telescopes from both generations.

At GEON, a first approach to obtaining local tie-vectors was to tag-along Ns to Ny in IVS R1-sessions and preliminary results have been reported by Kirkvik et al. (2021). However, most experiments used by Kirkvik et al. (2021) happened to be problematic due to technical failures such as malfunctioning recording systems, malfunctioning elevation encoder, warm receiver, etc. To obtain better data, and avoid tag-along constraints on bandwidth and scheduling, a dedicated experiment series called NYTIE was started.

Traditionally, IVS group-delay observations have uncertainties on the cm-level. While Varenius et al. (2021) and Xu et al. (2023) claim high precision, especially with phase delays, they do not compare their ONTIE or Ny-Ns results with other independent methods. Niell et al. (2021) find agreement between VLBI and an independent optical survey within about 1 mm, although for a very short (31 m) baseline. On the significantly longer NYTIE baseline, we are more sensitive to errors modeling differential atmospheric effects. Therefore, we expect larger NYTIE uncertainties of a few mm in the horizontal and about 1 cm in the vertical.

2. Instrumentation and Experimental Setup

Ny (Figure 1b) was an az-el mount legacy S/X telescope with a prime-focus antenna of 20 m diameter, designed for observations on S (2.2–2.5 GHz) and X band (8–9 GHz). Ns and Nn (Figure 1a) are az-el mount VGOS telescopes with a ringfocus antenna of 13.2 m diameter. The key differences of the two telescope generations are the broad band receivers on VGOS (2–14 GHz, which includes the X band), the use of linear polarisation instead of circular, and their ability for much faster slewing to gain more time actually spent on observing the radio sources. For more detailed differences, the reader is referred to Petrachenko et al. (2012). It is sometimes possible to mount an S/X receiver in a VGOS telescope, and Ns was equipped with an S/X band receiver for observations during the time of the NYTIE project. Nn was equipped with a regular VGOS receiver with a frequency range from 2 to 14 GHz. For more technical details about the telescopes' individual equipment the reader is referred to Garcia-Espada et al. (2023). The baseline Ny-Nn is slightly longer than the baseline Ny-Ns (1.62 km resp. 1.53 km). Nn and Ns are about 85 m apart.

The NYTIE experiments were conducted between March 2022 and August 2023, as a total of 23 short-baseline local interferometry sessions of 24 hr duration each were carried out with the two telescopes Ns and Ny (cf. Table 1). The first experiment was scheduled with *sked* (Gipson, 2018) using the source list of the IVS R1 experiment r11026. All following experiments were not scheduled anew, but used the same schedule which was rotated, that is, adjusted to the time of visibility of the radio sources. Using the same schedule shifted in time could potentially introduce systematics due to, for example, similar deficiencies in sky coverage. However, for these three close by telescopes this schedule provided very good sky coverage with no obvious deficiencies. Systematic source-structure related errors, which could arise since we are using the same set of sources in all schedules, are not significant on these short baselines (which do not resolve the sources).

A typical IVS 24-hr session that involves both Ny and Ns includes about 200 scans on this baseline in the years 2022 and 2023. For comparison, for our dedicated sessions about 800 scans are scheduled on the same baseline. This increased number of scans is due to the adaptation and optimisation of the schedule to the network of Ny, Ns, and Nn only, which means, for example, no idle time when waiting for other telescopes that are slewing very slowly or that are observing a radio source not visible from Ny-Ålesund. However, in practice we mostly did not get all 800 scans due to technical problems. On average, we had about 72% of good quality scans after correlation, ranging from 30% to 99%. NYTIE experiments were observed when it was possible, in between the IVS sessions, and when both Ny and Ns (and later also Nn) were functional to participate. Decisions about when to run the experiments were taken by the station leader S. Garcia-Espada, depending on the telescopes' availabilities. The number of sessions was intensified when the dismantling of Ny came closer. However, due to a number of different reasons including technical problems and a very low number of scans (<50), not all of these experiments are actually useful for a reliable analysis.

For NYTIEs only the frequencies between 8352.99 and 8932.99 MHz in the X band are analyzed. Measurements in S band are not considered necessary on the short baseline, as the influence of the ionosphere is assumed to be the same for the involved telescopes (see Section 4.5). Also, the data quality of X band is generally much better than that of S band due to less Radio Frequency Interference (RFI), hence we use X band only. The frequencies were also chosen as a parallel set-up to the ONTIE experiments (Handirk et al., 2023; Varenius et al., 2021), in prospective of including also Nn with VGOS-equipment at a later point in time. The overlap of the different technical equipment restricts the range of observation frequencies. The observation frequencies are listed in Table 2, which shows that two different frequency configurations have been used for NYTIE experiments.

Since March 2023, there are also 9 experiments in which Nn was additionally involved. This means that observations with all three telescopes can take place exclusively in the X band range, and that analyzing the data with a mixed-polarisation basis (e.g., right circular to X/Y-linear) as described by Varenius et al. (2021) is required. The basic concept is that we correlate for example, right-polarisation data from one telescope (with a circular S/X-receiver) with horizontal-polarisation data from another telescope (with a VGOS receiver). This is possible in a simple way as long as the telescopes are close together, so that their relative polarisation angles toward the sky do not change significantly during observations. More details about the combination of different

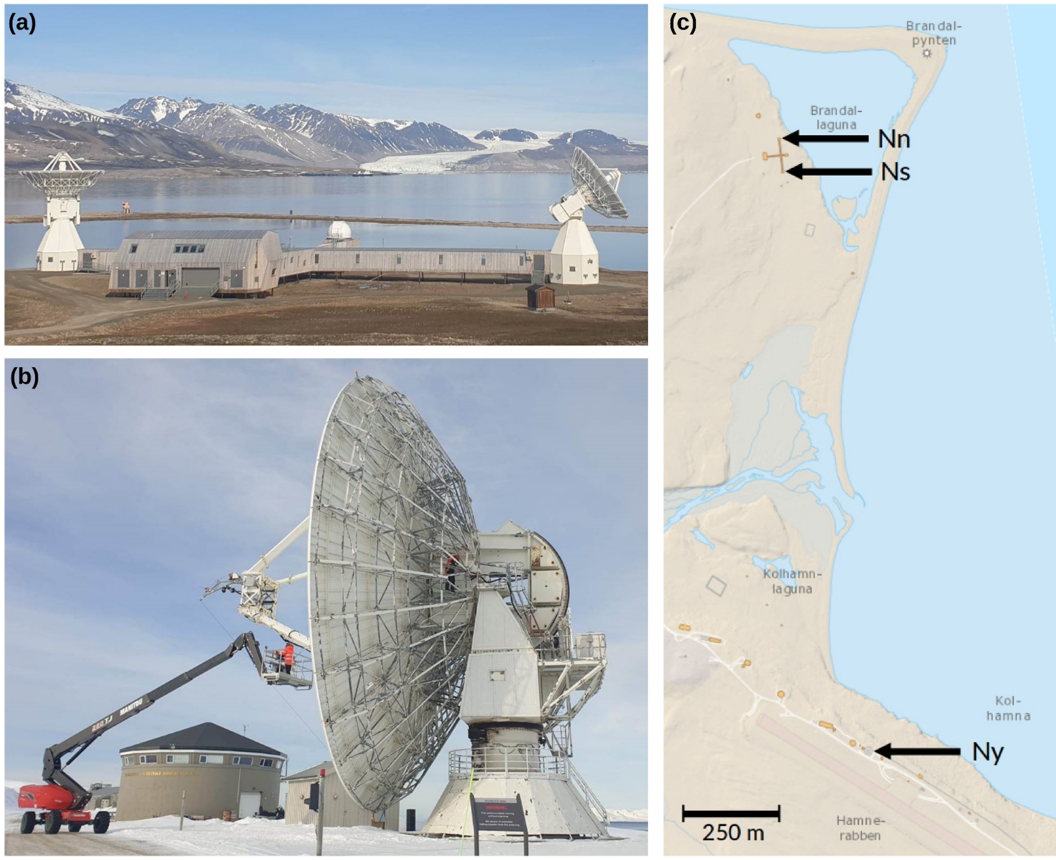

Figure 1. Telescopes at Ny-Ålesund used for NYTIEs: (a) New telescopes Nn (left, VGOS equipment) and Ns (right, S/X equipment). The baseline between these telescopes is ca. 85 m. Credit: S. Garcia-Espada/Kartverket. (b) S/X legacy telescope Ny. Credit: S. Garcia-Espada/Kartverket. (c) Map over the area of the Ny-Ålesund VLBI station (Norwegian Polar Institute, 2025).

polarisation signals can be found in Martí-Vidal et al. (2016). We analyzed the data in a similar way to the Australian Mixed Mode (AMM) (McCallum et al., 2022), that is, the telescopes with S/X equipment observe also on S band, but the recorded data is not used for correlation or analysis.

Furthermore, additional data were collected between Ns, Nn, and Ny by adding Ns and Nn along to Ny to regularly scheduled S/X IVS experiments. This was initially done for testing purposes of the telescope Ns, but results can also be used to analyze the local tie vectors at Ny-Ålesund. From these sessions, a selection of 33 IVS-R1, IVS-R4, IVS-RD and IVS-RDV experiments are used to complement the dedicated NYTIE time series, aiming for creating an approximately equally spaced time series with one to two experiments per fortnight. Those experiment types will be referred to as R1, R4, RD, and RV resp. hereafter and in Table 4. The reader may access the time line of the experiments through Tables 1 and 4, as well as Figure 2. Generally, these IVS experiments are referred to below with the abbreviation TA (tag-along) in order to distinguish them from the actual NYTIEs. A subset of these was already analyzed by Xu et al. (2023). Our selection was based on the comments in the IVS correlator and analysis reports, which include essential notes for each session, detailing, for example, hardware failures and correlation quality and can be found at the IVS Coordinating Center website. Despite the theoretically large amount of experiments to choose from, numerous problems reduce the availability of sessions. Some problems such as wrong time stamps in the data or many non-detections in X band (often ≥70%) led to the Ny-Ålesund baselines being excluded from correlation and/or analysis. Other issues like recording with a warm receiver, weak fringes, as well as reduced observation time due to late start or halt during the experiment further decrement the number of experiments that we expect to yield reasonable and high quality results. The quality of the available data is often further reduced by the influence of RFI: Around the Ny-Ålesund Research Station there are restrictions on the use of radio frequencies in the frequency range 2–32 GHz in the geographical area within a 20 km radius to protect

Table 1
Summary of the NYTIE Databases Analyzed in This Work

Exp. code	vgosDb	Config. (Table 2)	Excluded channels	Stations	WRMS (gd)	WRMS (pd)
ny2075	22MAR16VN	A	–	Ny, Ns	41 ps	22 ps
ny2080	22MAR21VN	A	–	Ny, Ns	32 ps	24 ps
ny2217	22AUG05VN	B	1, 2	Ny, Ns	64 ps	19 ps
ny2221	22AUG09VN	B	1, 2	Ny, Ns	67 ps	17 ps
ny2229	22AUG17VN	A	1, 2	Ny, Ns	60 ps	23 ps
ny2236	22AUG24VN	A	1, 2, 7	Ny, Ns	53 ps	20 ps
ny2242	22AUG30VN	A	1, 2	Ny, Ns	46 ps	16 ps
ny2243	22AUG31VN	A	1, 2	Ny, Ns	42 ps	17 ps
ny2263	22SEP20VN	A	1, 2	Ny, Ns	55 ps	16 ps
ny2270	22SEP27VN	A	1, 2	Ny, Ns	59 ps	16 ps
ny2271	22SEP28VN	A	1, 2	Ny, Ns	44 ps	19 ps
ny2276	22OCT03VN	A	1, 2	Ny, Ns	43 ps	18 ps
ny2278	22OCT05VN	A	1, 2	Ny, Ns	43 ps	28 ps
ny3076	23MAR17VN	A	1, 2	Ny, Ns, Nn	–	–[a]
ny3088	23MAR29VN	A	1, 2	Ny, Ns, Nn	55 ps	19 ps[b]
ny3109	23APR19VN	A	1, 2	Ny, Ns, Nn	45 ps	22 ps
ny3164	23JUN13VN	A	1, 2	Ny, Ns, Nn	57 ps	24 ps
ny3182	23JUL01VN	A	1, 2	Ny, Ns, Nn	50 ps	22 ps
ny3189	23JUL08VN	A	1, 2	Ny, Ns, Nn	49 ps	25 ps
ny3199	23JUL18VN	A	1, 2	Ny, Ns, Nn	45 ps	27 ps
ny3206	23JUL25VN	A	1, 2	Ny, Ns, Nn	39 ps	31 ps
ny3213	23AUG01VN	A	1, 2	Ny, Ns, Nn	45 ps	29 ps
ny3215	23AUG03VN	A	1, 2	Ny, Ns, Nn	50 ps	15 ps

Note. "gd" for group delay, "pd" for phase delay WRMS. [a]database fully excluded from analysis due to extremely short observation time and large outliers in resulting station coordinates. [b]Ns excluded from further analysis due to extremely short observation time and large outliers in resulting station coordinates.

VLBI observations from RFI. While the general rule is to avoid using equipment that emits radio frequencies, such equipment may be used for safety, operational, and scientific reasons under certain circumstances. Despite these regulations, unintentional RFI remains a concern. This is primarily due to the widespread presence of personal electronic devices with embedded radio transmitters (e.g., Bluetooth), combined with limited user awareness of their emission characteristics or how to disable them. Additionally, from May to September, many cruise ships are in the area, even in direct line of sight of the telescopes. These ships use several radio technologies, such as radar, and some also illegally provide Wi-Fi to their passengers through satellite technology within the protected zone. Both Wi-Fi and Bluetooth cause RFI and thus reduce the data quality. Since the appointed IVS analysts need the S band data for properly processing X band data, observations with low quality S band data are often excluded from analysis. Our selection of TA experiments for this study disregarded sessions where the appointed IVS centers commented on severe problems with one or more of the Ny-Ålesund telescopes.

Table 2
List of Frequency Configurations, Denoting the Lower Edge of Each Correlated BBC-Channel With the Bandwidth 16 MHz

BBC channel	Conf. A	Conf. B
1	8212.99	8212.99
2	8252.99	8252.99
3	8352.99	8352.99
4	8512.99	8512.99
5	8732.99	8732.99
6	8852.99	8852.99
7	8892.99	8912.99
8	8932.99	8932.99

Note. Frequencies given in MHz.

3. Analysis

The correlation and post-correlation processing of the NYTIE session data followed the same steps as described in Sections 4.1–4.4 in Varenius et al. (2021). In order to keep this article concise, we refer the reader to that article. However, we used newer versions of correlation software package

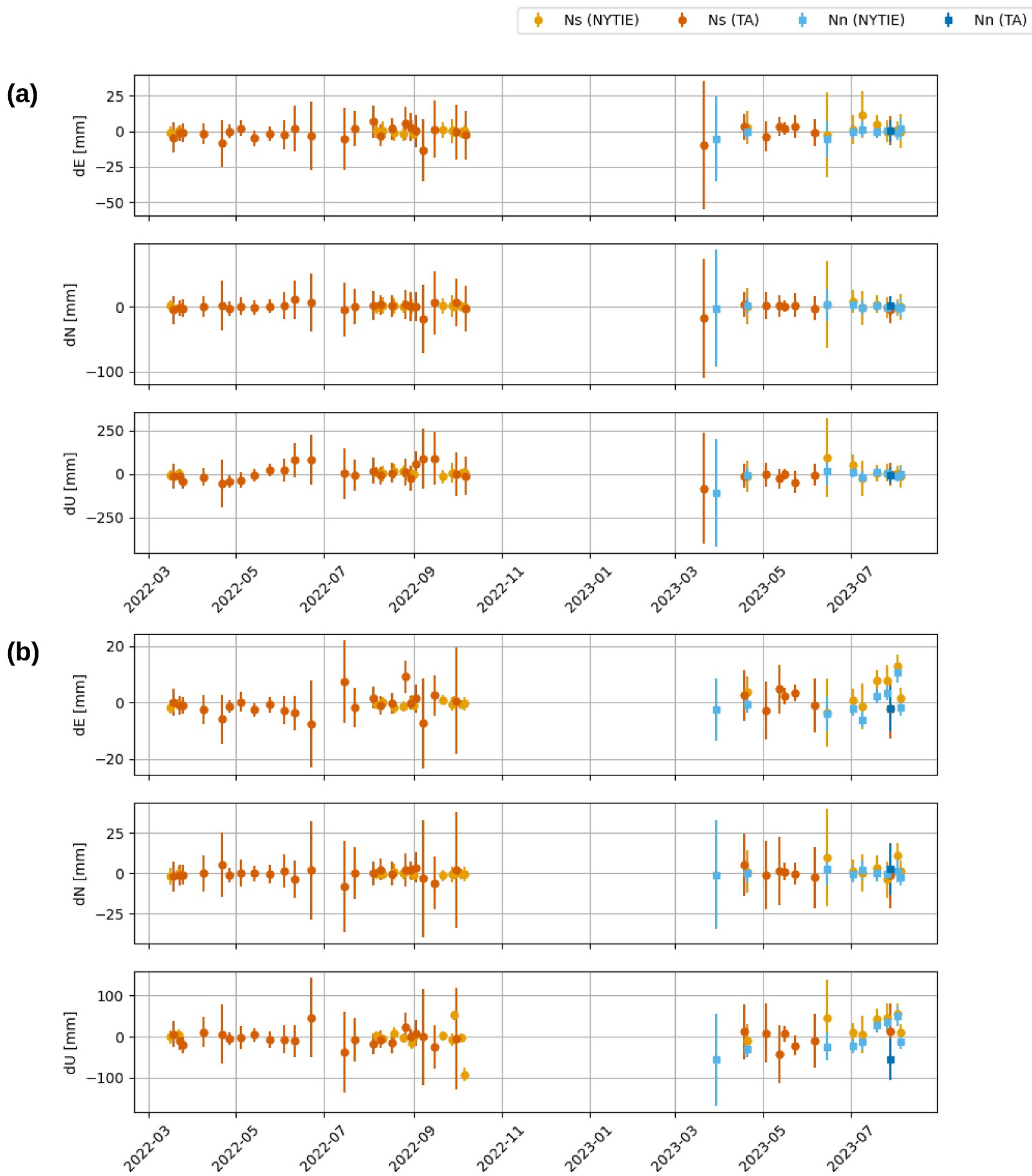

Figure 2. Group-delay (a) and phase-delay (b) position residuals for Ns and Nn with 3-σ uncertainties from all sessions (NYTIE + TA). Values are reduced by the weighted mean value. Uncertainties derived from formal 1-σ uncertainties reported by ASCoT. Orange hues used for Ns, blue hues used for Nn. Lighter shades indicate NYTIE experiments, darker shades indicate TA experiments.

DiFX (version 2.6.3) (Deller et al., 2011) and fringe-fitting software package HOPS fourfit (version 3.23) (MIT/Haystack, 2020). The analysis was done with ASCoT (version with git hash 15db0cb from repository https://github.com/varenius/ascot, Artz et al. (2016)). Standard physical models such as tidal corrections are included in the software, and extra noise is added automatically by the software in order to avoid overly optimistic results. We use the OSO2023X_TRF coordinates for all three telescopes Ny, Ns, and Nn as a-priori values for our analysis (cf. Table 3), and ICRF3 as realization of the ICRS. However, the values for Ns and Nn in the OSO2023X_TRF stem from a few TA measurements. Due to the small number of observations contributing to the specific TRF used, reliable velocities cannot be estimated for Ns and Nn. Therefore, Ny velocities are used to transfer coordinates from the TRF reference epoch to the experiment epochs. OSO2023X_TRF is a reference frame calculated from VLBI data 1979–2023 (the Onsala Space Observatory (OSO) solution to IVS), and is a reference frame aligned to

Table 3
Apriori Coordinates for the Telescopes Ny, Nn, Ns in OSO2023X_TRF, Reference Epoch 2015.0

	X (m)	Y (m)	Z (m)
Ny	1202462.485	252734.547	6237766.216
Nn	1200992.693	252098.644	6238038.622
Ns	1201070.663	252129.324	6238022.478

ITRF2020, obtained using No-Net-Translation/No-Net-Rotation. All the databases processed and analyzed are in the vgosDb file format. For more details on the format, see Gipson et al. (2014).

When analyzing with ASCoT, we fix Ny to its apriori position and only estimate the coordinates of Ns and Nn, with Ny serving as the reference station in each case. For the Zenith Wet Delay (ZWD) estimation, we use the VMF3 model (Landskron & Böhm, 2018), with data obtained from the VMF Data Server (VMF Data Server, 2026). In intervals of 20 min, the ZWD is estimated for Ns and Nn, but not estimated for Ny. Due to the short baseline length, it is practically impossible to estimate the ZWD for all three telescopes. With the estimation setup used, we estimate the difference in ZWD between Ny and Ns resp. Nn. We calculated a priori tropospheric gradients using the APG (A Priori Gradient, (Böhm et al., 2013)) model, however no gradients are estimated in the analysis as gradients are not expected to be an issue on such short baselines. Using the a priori model should correct for any systematic differences. We also apply telescope models to account for thermal as well as gravitational deformation. The data processing strategy described above is referred to as version 1 in our discussion in Section 4.3, in which the impact of these analysis components is investigated.

It was found during post-correlation and analysis that the two lowest channels (8212.99 and 8252.99 MHz) are often strongly influenced by RFI. We therefore generally dispense with these two channels and restrict ourselves to the fourfit channels 3–8 mentioned in Table 2, except for the very first sessions (cf. Table 1). TAs were scheduled by the appointed IVS Operation Centers, with Ns and Nn tagged along to Ny in each case. Correlation and analysis were thus also in the hands of the centers officially appointed by the IVS. In our analysis, we therefore concentrate on those TAs for which the correlator resp. Analysis reports show that there were no severe problems with the involved telescopes of the GEON nor with the baselines between them, and we re-analyze them with ASCoT focusing exclusively on the baselines Ny-Ns and Ny-Nn. We analyze both X-band delay observables: the group delay (gd) and the phase delay (pd). The vgosDbs supplied by the IVS contain group delays which we can use directly, so we do not need to re-analyze these. However, phase delays require the phase ambiguities to be resolved, and since the appointed IVS analysis centers by default do not resolve them (resolving phase ambiguities in general is not possible for long baselines), we had to solve the ambiguities for all databases. This step was completed on the basis of the latest wrapper file in the published vgosDb. For experiments in 2022, we solved the ambiguities in νSolve (Bolotin et al., 2014) and in some cases refined the result with the solve_ambiguities module in ASCoT. For experiments in 2023, we only used ASCoT.

In order to be able to compare and combine the results from each individual session, we transform the results to the reference epoch 2023.0 using the station velocities for Ny from the OSO2023X_TRF (X, Y, Z):

$$v_{Ny} = \begin{bmatrix} -0.0115 \\ 0.0045 \\ 0.0165 \end{bmatrix} \mathrm{m/y}$$

We assume that all three telescopes move with the same velocity and the same direction.

4. Results and Discussion

In this section we present the results of our analysis and discuss the findings with respect to our aims and modeling.

4.1. Station Coordinates

The resulting tie-vectors from Ny to Ns and Nn are presented in Table 5 (group delay results) and 6 (phase delay results). The differences between solutions based on only NYTIE, only TA or both combined are a few mm. However, best results in terms of precision are yielded when combining NYTIE and TA experiments as this enlarges the total number of experiments. Hence, we refer only to results from combined NYTIE and TA hereafter. The local tie vectors in ITRF2020 (X, Y, Z) from the combined data sets from group delay results are:

10.1029/2025RS008586

Table 4
Summary of the TA Databases Analyzed in This Work

vgosDb	Type	Correlator center	Stations	WRMS (gd)	WRMS (pd)
22MAR17XE	R4	Wash	Ny, Ns	55 ps	25 ps
22MAR22XA	R1	Bonn	Ny, Ns	39 ps	22 ps
22MAR24XE	R4	Wash	Ny, Ns	40 ps	18 ps
22APR07XE	R4	Wash	Ny, Ns	38 ps	26 ps
22APR20XB	RD	Shao	Ny, Ns	44 ps	23 ps
22APR25XA	R1	Bonn	Ny, Ns	38 ps	17 ps
22MAY03XA	R4	Bonn	Ny, Ns	39 ps	24 ps
22MAY12XE	R1	Wash	Ny, Ns	42 ps	18 ps
22MAY23XA	R4	Bonn	Ny, Ns	34 ps	18 ps
22JUN02XE	R4	Wash	Ny, Ns	58 ps	28 ps
22JUN09XE	R4	Wash	Ny, Ns	61 ps	21 ps
22JUN21XA	R1	Bonn	Ny, Ns	21 ps	13 ps
22JUL05XA	RV	VLBA	Ny, Ns	33 ps	20 ps[a]
22JUL14XE	R4	Wash	Ny, Ns	57 ps	35 ps
22JUL21XE	R4	Wash	Ny, Ns	53 ps	29 ps
22AUG03XE	R4	Wash	Ny, Ns	51 ps	16 ps
22AUG08XA	R1	Bonn	Ny, Ns	53 ps	21 ps
22AUG16XA	R1	Bonn	Ny, Ns	50 ps	23 ps
22AUG25XE	R4	Wash	Ny, Ns	60 ps	26 ps
22AUG29XA	R1	Bonn	Ny, Ns	64 ps	15 ps
22SEP01XE	R4	Wash	Ny, Ns	65 ps	26 ps
22SEP06XA	RV	VLBA	Ny, Ns	63 ps	50 ps
22SEP14XA	RD	Wash	Ny, Ns	70 ps	50 ps
22SEP29XE	R4	Wash	Ny, Ns	74 ps	23 ps
22OCT06XE	R4	Wash	Ny, Ns	78 ps	64 ps[b]
22OCT31XA	R1	Bonn	Ny, Ns	10 ps	26 ps[a]
20230320-r11095	R1	Bonn	Ny, Ns	58 ps	48 ps[b]
20230323-r41095	R4	Wash	Ny, Ns	39 ps	26 ps[a]
20230417-r11099	R1	Bonn	Ny, Ns	52 ps	49 ps
20230502-r11101	R1	Bonn	Ny, Ns	44 ps	46 ps
20230511-r41102	R4	Wash	Ny, Ns	26 ps	34 ps
20230515-r11103	R1	Bonn	Ny, Ns	25 ps	16 ps
20230522-r11104	R1	Bonn	Ny, Ns	47 ps	17 ps
20230531-r41105	R4	Wash	Ny, Ns	77 ps	21 ps[c]
20230605-r11106	R1	Bonn	Ny, Ns	59 ps	55 ps
20230614-r41107	R4	Wash	Ny, Ns	59 ps	41 ps[c]
20230727-r41113	R4	Wash	Ny, Ns, Nn	40 ps	40 ps

Note. "gd" for group delay, "pd" for phase delay WRMS. WRMS only for analyzing Ny, Ns, Nn, but not the entire network. [a]database fully excluded from further analysis due to very large uncertainties in gd and pd. [b]pd results excluded from further analysis due to large outliers in resulting station coordinates. [c]database fully excluded from further analysis due to large outliers in resulting station coordinates and large uncertainties.

10.1029/2025RS008586

Table 5
Weighted Mean Local Tie Vector Components From Ny in ITRF2020 at Epoch 2023.0 for Ns and Nn From Group Delay Results

Data	ΔX (m)	ΔY (m)	ΔZ (m)	σ_X (mm)	σ_Y (mm)	σ_Z (mm)
Ns (21 NYTIE, 33 TA sessions)						
only NYTIE	−1391.8161	−605.2271	256.2461	0.6	0.4	2.5
only TA	−1391.8183	−605.2278	256.2344	0.8	0.5	3.5
NYTIE + TA	−1391.8168	−605.2274	256.2422	0.5	0.3	2.0
Nn (9 NYTIE, 1 TA session)						
only NYTIE	−1469.7799	−635.9252	272.3943	0.9	0.6	3.9
only TA	−1469.7832	−635.9258	272.3882	3.8	2.4	16.1
NYTIE + TA	−1469.7801	−635.9252	272.3939	0.9	0.5	3.8

Note. Formal 1-σ uncertainties as reported by ASCoT were used to calculate the weighted means.

$$b_{NyNs} = \begin{bmatrix} -1391.8168 \\ -605.2274 \\ 256.2422 \end{bmatrix} \text{m} \pm \begin{bmatrix} 0.5 \\ 0.3 \\ 2.0 \end{bmatrix} \text{mm}$$

$$b_{NyNn} = \begin{bmatrix} -1469.7801 \\ -635.9252 \\ 272.3939 \end{bmatrix} \text{m} \pm \begin{bmatrix} 0.9 \\ 0.5 \\ 3.8 \end{bmatrix} \text{mm}$$

The uncertainties given here are the formal 1σ propagated when forming the weighted averages from each epoch-uncertainty as given by ASCoT; as shown in Section 4.2, these formal uncertainties are over-optimistic, and final uncertainties are given in Table 8. Comparing to the ONTIE series (Varenius et al., 2021), the majority of experiments used in this study are not dedicated experiments, that is, that we generally have more experiments that were not optimized for the network of Ny, Ns, Nn only, and that we have much less scans per baseline. This leads to slightly less accurate results per session, and a larger scatter of individual experiment results.

Figure 2 shows results of NYTIE experiments in yellow and light blue, and of TAs in orange and dark blue, including their respective 3-sigma error bars. It is noticeable that especially the results of the NYTIEs in 2022 scatter significantly less and have better uncertainties. For each coordinate component, the weighted mean has been subtracted from all results, thus the mean is always at 0 mm displacement. Notably, the differences for the Up-component results and their associated uncertainties are comparatively large.

For Nn, the differences between group and phase delay solutions, but also between the different sets differ more than in the case of Ns. However, the total number of sessions with Nn is 10 experiments, which also reflects in the uncertainties.

Figure 3 shows that the results of the NYTIEs for station Ns are better than those of the TAs, especially in 2022. This is not so apparent in 2023, where the results of the NYTIEs are worse than in 2022 and are more in line with

Table 6
Weighted Mean Local Tie Vector Components From Ny in ITRF2020 at Epoch 2023.0 for Ns and Nn From Phase Delay Results

Data	ΔX (m)	ΔY (m)	ΔZ (m)	σ_X (mm)	σ_Y (mm)	σ_Z (mm)
Ns (21 NYTIE, 30 TA sessions)						
NYTIE + TA	−1391.8151	−605.2272	256.2528	0.2	0.1	0.9
Nn (9 NYTIE, 1 TA session)						
NYTIE + TA	−1469.7781	−635.9238	272.4163	0.5	0.3	2.2

Note. Formal 1-σ uncertainties as reported by ASCoT were used to calculate the weighted means.

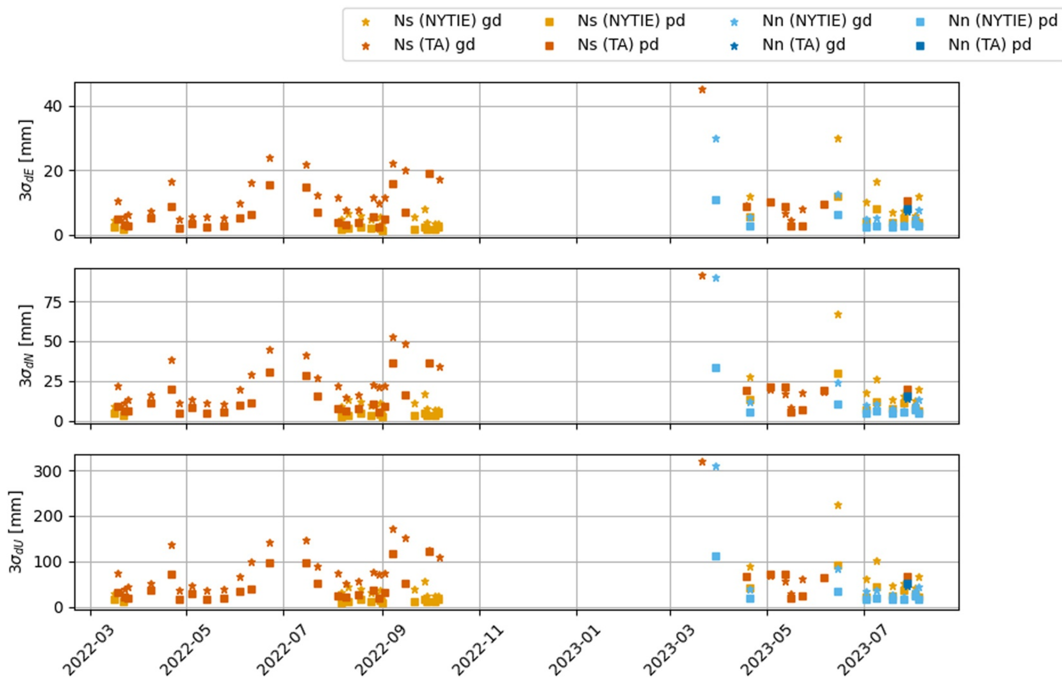

Figure 3. Comparison of 3-σ uncertainties yielded from all NYTIE and TA experiments, derived from formal 1-σ uncertainties reported by ASCoT. Orange used for Ns, blue for Nn. Asterisks represent group delay results, squares phase delay results. Light colors used for NYTIE experiments, dark colors for TA experiments.

those of the TAs in 2022. The results of the TAs in 2023, on the other hand, have not become any worse, but are comparable to those of 2022. This comparison cannot be made for station Nn. The data of the TA experiments, if available at all, are rarely of sufficient quality and quantity, so that we only consider one single TA experiment at all for Nn. Its precision is similar to that for Ns in TAs, and comparable to the NYTIEs in the horizontal components. It is slightly worse for height. A similar behavior is seen in the WRMS of the individual experiments (cf. Tables 1 and 4): The results are generally better for NYTIEs than for TAs.

Table 7 presents the weighted mean local tie vector components between Ny and Ns resp. Nn for group and phase delays in a local ENU frame. We use the reference point of Ny as the ENU origin and the vector direction Ny → Ns. The survey values included in the table stem from the classical geodetic survey described in Section 4.2.

Comparing our group and phase delay results, we find a difference of about 1 cm in the Up-component for Ns. The origin of this difference is investigated in Section 4.3, and a comparison with independent VLBI results for the same baseline is given in Section 4.4.

4.2. Comparison to Local Ties From Total Station and GNSS

In order to validate either group or phase delay results, we compare our weighted mean local tie vectors Ny-Ns and Ny-Nn to the results of a classical geodetic survey from 2023, which are also given in Table 7. The Norwegian Mapping Authority Kartverket conducted this local tie survey with total station (Leica TS 15) between reference points at Ns and Nn and other control markers annually since 2018. In summer 2023 the reference point of Ny was included in the survey. The reference point of a VLBI telescope is defined to be the invariant point of the telescope, that is, a point within the structure of a telescope which is invariant to any rotations of the telescope (Nothnagel, 2025). The invariant points for all three VLBI telescopes in Ny-Ålesund were determined by outside prisms and by moving the dish around the horizontal and vertical axes. The reference points of Ns and Nn were additionally determined by local markers inside the azimuth cabin determined by the manufacturer Asturfeito. The stations in the network were connected to ITRF2020 by the coordinates of the IGS station NYA1 and the

Table 7
Weighted Mean Local Tie Vector Components for Group (gd) and Phase Delay (pd) Results From all Sessions (NYTIE + TA), and From the Classical Geodetic Survey by Kartverket in Summer 2023

	ΔE (m)	ΔN (m)	ΔU (m)	$\sigma_{\Delta E}$ (mm)	$\sigma_{\Delta N}$ (mm)	$\sigma_{\Delta U}$ (mm)
Ns, VLBI gd	−306.0082	1508.0845	−33.9775	0.3	0.6	2.0
Ns, VLBI pd	−306.0084	1508.0848	−33.9668	0.1	0.3	0.9
Ns, survey	−306.0075	1508.0844	−33.9702	0.3	0.3	0.4
Nn, VLBI gd	−320.0136	1592.2590	−33.9895	0.5	1.1	3.7
Nn, VLBI pd	−320.0127	1592.2611	−33.9672	0.3	0.6	2.2
Nn, survey	−320.0136	1592.2587	−33.9905	0.3	0.3	0.4

orientation was ensured by utilizing the IGS station NABG, close to Ns and Nn. The local-tie observations were analyzed with the least-squares adjustment software COMP3d v5.19 from IGN France (Damien Pesce, private communication). For more details, see Tangen et al. (2024). It is also worth noting that none of the yearly surveys indicated instabilities exceeding a few millimeters between the three VLBI telescopes, or between the VLBI telescopes and the other main geodetic instruments in Ny-Ålesund (Tangen et al., 2024).

We find that the weighted mean of the group and phase delay results agrees well with the survey results at the level of the estimated values. However, when considering the formal uncertainties, several discrepancies become statistically significant. For example, the difference between the group delay result for Ns (-33.9775 ± 0.002 m) and the Kartverket survey (-33.9702 ± 0.0004 m) amounts to -7.3 ± 2.0 mm, corresponding to approximately 3.6σ when combining the uncertainties in quadrature. Similar behavior is observed for the difference between the phase delay result for Ns and the Kartverket survey which is at the level of 3σ.

In the case of Nn, the difference between the group delay result and the Kartverket survey remains within 1σ and is therefore not statistically significant, while the difference between the phase delay result and the Kartverket survey reaches about 10σ. However, these statistics are based on a low number of experiments and should be taken with precautions.

We interpret the discrepancy between the well-established local survey results and these short-baseline VLBI observations as evidence of over-optimistic formal errors for the VLBI results. This is supported by the internal consistency of our own data: the scatter of the individual session positions (cf. Figure 2) and the differences between session types found in Section 4.3 both indicate session-dependent systematic effects of several millimeters in the Up component. The over-optimism can be quantified from the repeatability of the results themselves: while the variance factors of the individual session solutions are close to unity, that is, the fits are internally consistent, the χ^2 per degree of freedom of the individual Up estimates about their weighted means is 1.6 and 13.4 for the Ns group and phase delay series, and 0.8 and 18.9 for Nn. The excess scatter is thus caused by effects that are stable within a session but change from session to session. Rescaling the uncertainty of each weighted mean by $\sqrt{\chi^2/\mathrm{dof}}$ yields Up uncertainties of 2.5, 3.3, 3.4, and 9.5 mm for Ns (gd, pd) and Nn (gd, pd), respectively; the nominal 10σ discrepancy of the Nn phase delay solution in particular reflects its strongly over-optimistic formal error rather than a correspondingly large offset.

Table 8
Final Weighted Mean Local Tie Vectors From Ny in ITRF2020 (X, Y, Z) at Epoch 2023.0 From all Sessions (NYTIE + TA), With Total 1-σ Uncertainties: The Formal Uncertainties Rescaled per Component to Match the Observed Session-to-Session Scatter, and the Adopted Residual Modeling Systematic of 7 mm in the Up Direction Projected Into (X, Y, Z) and Added in Quadrature

	ΔX (m)	ΔY (m)	ΔZ (m)	σ_X (mm)	σ_Y (mm)	σ_Z (mm)
Ns, VLBI gd	−1391.8168	−605.2274	256.2422	1.4	0.4	7.3
Ns, VLBI pd	−1391.8151	−605.2272	256.2528	1.4	0.4	7.6
Nn, VLBI gd	−1469.7801	−635.9252	272.3939	1.5	0.5	7.7
Nn, VLBI pd	−1469.7781	−635.9238	272.4163	2.1	1.7	11.6

Table 9
Different Versions of Analyzing the NYTIE Experiments

Version	Thermal Def. Modeling	Gravit. Def. Modeling	ZWD estimation	Interval for pwl clock estimation
1	all	all	Ns, Nn	60 min
2a	none	all	Ns, Nn	60 min
2b	Ny	all	Ns, Nn	60 min
2c	Ns, Nn	all	Ns, Nn	60 min
3a	all	none	Ns, Nn	60 min
3b	all	Ny	Ns, Nn	60 min
3c	all	Ns, Nn	Ns, Nn	60 min
4	all	all	none	60 min
5	all	all	Ns, Nn	20 min

With the rescaled uncertainties, the differences with respect to the survey correspond to 2.9σ, 1.0σ, 0.3σ, and 2.5σ. Consistency at the 2σ level requires an additional modeling systematic of at least 2.6 mm for the Ns group delay and 6.7 mm for the Nn phase delay solution, while the other two require none; we therefore adopt a residual modeling systematic of 7 mm, with which all four solutions agree with the survey at the 2σ level. This value is consistent with the roughly 10 mm budget for gravitational deformation modeling errors and uncalibrated instrumental delay variations estimated by Niell et al. (2021). Errors common to both observables, such as the telescope reference point or uncalibrated instrumental delays, cancel in the *difference* between the group and phase delay solutions; the group–phase delay difference therefore isolates the observable-specific part of these errors. We investigate its origin in the following subsection. Table 8 summarizes the final local tie vectors in ITRF2020 (X, Y, Z) with these total uncertainties.

4.3. Effects of Modeling Telescope Deformation, ZWD, and Clock on the Group–Phase Delay Difference

In Section 4.1 we found a significant difference between the group and phase delay solutions, reaching about −10 mm in the Up component for Ns. In contrast to the comparison with the survey results (Section 4.2), this difference is insensitive to errors that are common to both solutions, such as the telescope reference point or uncalibrated instrumental delays. It must instead be caused by something that affects the group and phase delay analyses *differently*. We therefore investigate which of our modeling choices, if any, couple differently to the two observable types. We expect the telescope deformation models as well as the ZWD estimation to have the largest effect on the Up-component (which, due to the extreme northern latitude, corresponds closely to the Z-component). Therefore, we analyzed all experiments in the versions listed in Table 9, for both group and phase delays.

Version 1 is our standard analysis, used for all results discussed in the sections above. For each version and each experiment we form the per-session difference $d = \mathrm{gd} - \mathrm{pd}$ of the estimated Ns position, and then the double difference $\Delta d = d_{\mathrm{version}} - d_{\mathrm{v1}}$. In the double difference all session-specific effects that are treated identically by the two solutions cancel, so Δd isolates the differential effect of the respective model on the group–phase delay discrepancy. All statistics below are based on the same 51 sessions (21 NYTIE, 30 TA) of the Ny-Ns baseline; we note that, to keep the same telescope configuration, Nn is included in all versions where present in the original data. However, due to the small number of experiments that include Nn, we only use the Ny-Ns baseline to evaluate the effects of the respective analysis version. Note that for Ny a gravitational deformation model is included in the file provided by the IVS Analysis Coordinator (AC) (IVS-AC, 2023). There are no models included in the same file for Nn or Ns. However, since they are of the same kind as the Onsala Twin Telescopes (OTT) we use the known deformation models of the OTT also for Nn and Ns from the IVS AC file.

For reference, the weighted mean of the per-session differences d in version 1 is -9.4 mm in the Up-component, with a formal 1-σ uncertainty of the mean of 2.3 mm (propagated from the ASCoT formal errors). Notably, this difference is not homogeneous across session types: it is -6.9 ± 2.7 mm for the NYTIE sessions but -15.1 ± 4.0 mm for the TA sessions.

Switching off the thermal deformation modeling (versions 2a–c) changes the individual coordinate solutions by up to a few tenths of a millimeter, and switching off the gravitational deformation modeling (versions 3a–c) by up to about 2 mm in Z for the group delays. However, these changes are almost identical for the group and the phase delay solutions: the double differences Δd in Up stay below 0.1 mm in the mean for every sub-version (largest: $+0.07 \pm 0.05$ mm, for one of the gravitational deformation sub-versions), with extremes below 0.25 mm for individual sessions. The deformation models are deterministic corrections to the modeled geometry and shift both solutions of a given session by the same amount. They therefore do not contribute to the observed group–phase delay difference, regardless of their absolute accuracy.

The ZWD estimation (version 4) behaves fundamentally differently. Here the double differences of individual sessions reach from -95 to $+72$ mm in Up, with 35 of the 51 sessions changing by more than 10 mm—yet with a mean of only $+0.3 \pm 5.1$ mm, that is, consistent with zero. Omitting the ZWD estimation thus scrambles the per-session group–phase delay differences dramatically, but without a coherent direction: the unmodelled wet delay of a given session propagates into the station height differently for the group and the phase delay solution, with sign and size depending on the actual atmospheric conditions. The troposphere is consequently the only tested analysis component to which the two observable types respond differently, which supports differential zenith wet delays as the most plausible cause of the group–phase delay discrepancy, as hypothesized in Section 4.1.

Shortening the clock parameterization interval from 60 to 20 min (version 5) changes the group–phase delay difference in Up by $+1.6$ mm on average (standard error 1.1 mm), with a session-to-session spread of 7.9 mm that is dominated by a single session (+55 mm); excluding it, the mean change is $+0.5 \pm 0.3$ mm with a spread of 1.9 mm. The clock parameterization thus couples only weakly to the group–phase delay difference, at a level an order of magnitude below the observed discrepancy.

In summary, the deformation models cancel in the group–phase delay difference at the 0.1 mm level and the clock parameterization couples to it only at the 1 mm level, while the treatment of the wet troposphere couples strongly, though incoherently, to it. Together with the session-type dependence of the mean difference (-6.9 mm for NYTIE vs. -15.1 mm for TA sessions, which differ in scheduling and observing geometry), this points toward the differential troposphere, rather than telescope modeling, as the origin of the height discrepancy between group and phase delay local ties.

4.4. Comparison With Other VLBI Local-Tie Results

Xu et al. (2023) determined the Ny-Ns baseline from 19 IVS sessions observed between May 2020 and June 2022, of which six are also part of our TA data set, and analyzed them independently with different software (νSolve). They report the reverse vector (Ns → Ny) with the ENU origin at Ns; comparing raw ENU components with our convention therefore shows apparent differences of up to 38 cm. Comparing the vectors in a common convention, that is, differencing them in XYZ and rotating the difference into the ENU frame at Ny, our phase delay vector agrees with their phase delay vector to $+1.1$ mm, -2.0 mm, and -5.1 mm in the East, North, and Up components—within 2σ of the combined uncertainties, using the rescaled uncertainties and residual systematics derived in Section 4.2, for two largely independent data sets and fully independent analyses.

Our group delay vector differs from theirs by -32 mm in Up, which remains significant even with the rescaled uncertainties. However, their own results show that their group delay solution is much less reliable than their phase delay solution for this baseline: the Up repeatability is 16 mm for group delays versus 4.7 mm for phase delays, an excess which Xu et al. (2023) attribute to problems with the phase calibration signals.

Xu et al. (2023) find a group–phase delay Up difference of similar magnitude to ours but of opposite sign (+16 mm vs. our -11 mm in the Ny → Ns sense). The group–phase delay difference is thus not a stable property of the baseline, but depends on the observing period, instrumentation, and analysis—consistent with the session-dependent tropospheric origin identified in Section 4.3.

Niell et al. (2021) find group and phase delay results for the very short 31 m baseline at Kokee to be consistent. Varenius et al. (2021) noted a small systematic difference between group and phase-delay vectors on the ~500 m ONTIE baselines. The magnitude of the group–phase delay discrepancy thus appears to grow with baseline length, as expected for a differential tropospheric effect, while its sign varies between data sets and analyses.

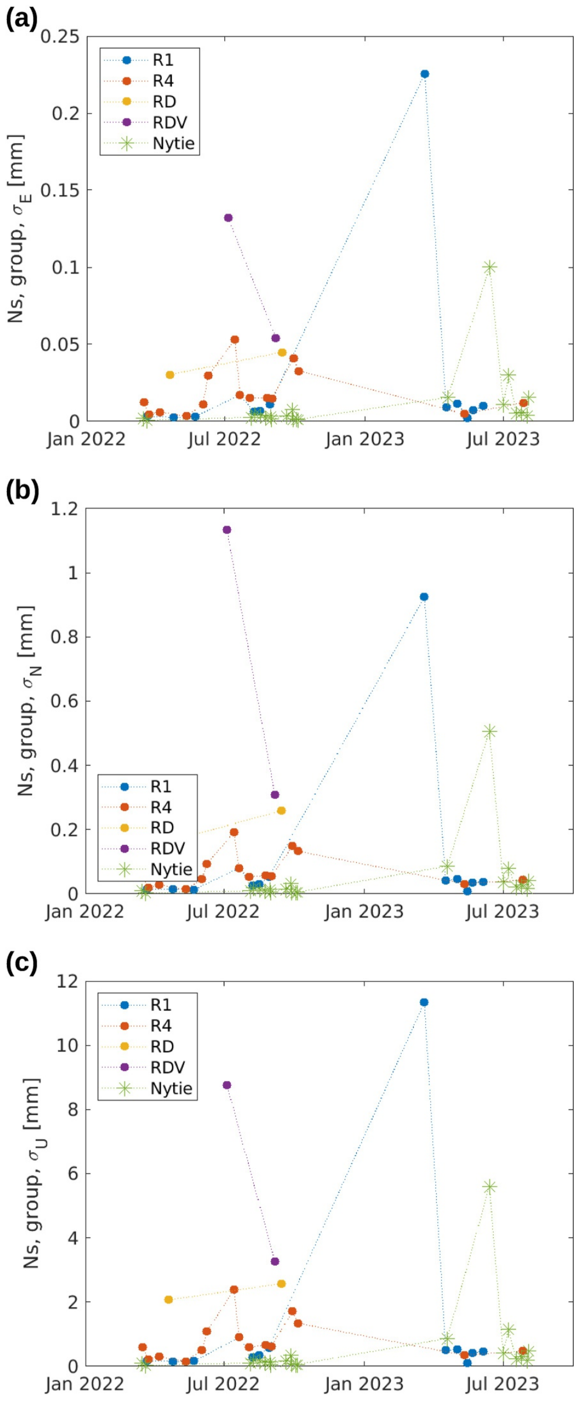

Figure 4. Comparison of yielded σ_E (panel a), σ_N (panel b), and σ_U (panel c) by experiment type for Ns from group delays results in (mm). Lines between data points only serve as visual aid.

4.5. Rationale for Neglecting the Ionosphere

In VLBI, the S-band delay is only used to correct the X-band delay for the dispersive effect of differential ionospheric TEC. As noted in Section 2 we assume no systematic differences in the ionosphere between Ns/Nn and Ny. There are several research articles which support this assumption, for example, Xu et al. (2023), Datta-Barua et al. (2002), Edwards (1987), and Niell et al. (2021). The short baselines significantly impact the ability for high-resolution ionosphere estimation from the interferometer data alone. However, as a test, we analyzed the group delays from all TA-sessions used in the paper from 2022 (26 sessions) which do have S-band data. We did two solutions, one applying the ionosphere correction (based on S- and X-band) and one without. On average the difference in the Z-coordinate is only about -1 mm (correcting for ionosphere–not correcting), with an uncertainty of ±1.5 mm. For phase delays we expect that the effect of the ionosphere should be of the same magnitude as for group delays but with opposite sign. Thus, the ionosphere would affect the difference between group and phase on the level of -2 ± 3 mm, which is much smaller than the observed group–phase delay difference of about 10 mm in Up (see Section 4.1).

Additional tests with ionospheric corrections based on GNSS TEC maps affected the Z-coordinate only on the 0.1 mm level. Therefore we conclude that, in agreement with literature, the discrepancies found (between group/phase-delays, and with respect to the Kartverket survey results) cannot be explained by the (lack of) ionosphere modeling.

4.6. Comparison of Experiment Types

As established in Section 4.1, we find that dedicated sessions perform better than TA's. However, as we use different types in the TA experiments (R1, R4, RV, RD), whose correlation and analysis results are based on different conditions, we can compare the uncertainties achieved for the station coordinates of Ns and Nn by type (cf. Figure 4) and determine if certain session types should be preferred for or excluded from analysis. In addition to the fact already mentioned that the NYTIEs generally perform better than the TAs, it is particularly clear that there is hardly any difference between the results of R1 and R4 experiments. This is advantageous for filling the gaps in our NYTIE time series, as these experiment types predominate in terms of numbers. Although the individual R1 and R4 experiments are not all of the same quality in terms of the availability and quality of the observations from the respective telescopes in Ny-Ålesund, there is more choice of available and of comparable quality TA experiments with which to supplement the NYTIE time series. As expected, RD and RV experiments do not contribute with comparable quality, as the purpose of these is dedicated to astrometry in contrast to geodesy. However, although these sessions have larger uncertainties, and hence do not contribute as much to the final weighted result, we included them as a consistency check during periods without NYTIE sessions.

5. Summary and Conclusions

The main outcome of the NYTIE project is the local tie vectors between Ny and Ns resp. Nn as presented in Section 4.1, with final uncertainties as summarized in Table 8. The phase delay results are in agreement, at the few-mm level, with the results of Xu et al. (2023), which are based on an independent analysis of a partially overlapping (six common sessions) data set. The station coordinate results from both NYTIE and TA sessions are very much comparable for the case of Ns, while the corresponding formal uncertainties are slightly better when using only NYTIEs compared to using only TAs.

As expected, the formal uncertainties are best when combining both session types, as this drastically enlarges the total number of experiments. This is very similar for the case of Nn, however, the total number of sessions is much smaller and hardly allows for a meaningful calculation of a mean value.

The results presented in Section 4.1 support the use of dedicated tie experiments instead of relying only on tagging Ns (and later Nn) along to Ny in the regular R1 and R4 experiments by the IVS. Consequently, we recommend observatories with several radio telescopes contributing to, for example, the ITRF to undertake dedicated VLBI local tie experiments. If dedicated tie experiments are not possible, tagging along to experiments scheduled for the regular IVS networks should be considered as a fall-back option. In case of tagging along, we recommend to prefer R1 and R4 sessions over experimental ones dedicated to research and development. It should be noted, however, that making use of IVS experiments likely requires some of the post-processing steps to be redone in order to treat phase ambiguities on the short baselines.

Comparing our VLBI vectors to established local survey results we find our formal uncertainties too optimistic, by up to a factor of four for the phase delay solutions. Rescaling the uncertainties to match the observed session-to-session scatter, and allowing for a residual modeling systematic of 7 mm, both group and phase delay results agree with the classical local survey at the 2σ level.

The offset between phase and group delay positions is investigated through sensitivity tests based on per-session double differences. Telescope deformation modeling (thermal and gravitational), while changing the individual positions by up to about 2 mm in the vertical component, affects group and phase delay solutions almost identically and thus cancels in their difference at the 0.1 mm level. In contrast, disabling the estimation of the zenith wet delay changes the group–phase delay difference of individual sessions by tens of millimeters in the vertical component, with session-dependent sign. The troposphere is thus the only tested analysis component to which the two observable types respond differently, and the most plausible origin of the observed group–phase delay discrepancy, whose magnitude and sign also vary between independent analyses of the same baseline (Xu et al., 2023). This highlights the critical importance of accurate tropospheric modeling in VLBI local tie analyses.

Conflict of Interest

The authors declare no conflicts of interest relevant to this study.

Availability Statement

All VLBI databases used in this work (NYTIE and tag-along sessions, in vgosDb format, including correlator and analysis reports) are publicly available from the data centres of the International VLBI Service for Geodesy and Astrometry (IVS) via https://ivscc.gsfc.nasa.gov/sessions/. The per-session tie vector results for Ns and Nn underlying Tables 5–7 are provided in machine-readable format in Handirk et al. (2026). The local tie survey values used for comparison are reproduced in full in Table 7; the underlying survey observations are held by the Norwegian Mapping Authority (Tangen et al., 2024). All software used in the analysis is publicly available: the databases were correlated with DiFX (version 2.6.3) (Deller et al., 2011) and fringe-fitted with HOPS fourfit (version 3.23) (MIT/Haystack, 2020); phase ambiguities were resolved with νSolve (Bolotin et al., 2014), available at https://sourceforge.net/projects/nusolve/; and the geodetic analysis was performed with ASCoT (Artz et al., 2016), available at https://github.com/varenius/ascot (git hash 15db0cb).

Acknowledgments

We thank the staff of the Ny-Ålesund Geodetic Earth Observatory and the Norwegian Mapping Authority (Kartverket) for operating the telescopes, carrying out the NYTIE observations, and conducting the local tie surveys. The results reported in this paper are based on data coordinated by the International VLBI Service for Geodesy and Astrometry (IVS); the data of the tag-along sessions were provided by the IVS, and we gratefully acknowledge the work of the IVS Operation Centres, correlators, and analysis centres. We thank the anonymous referees, whose comments significantly improved the manuscript.

References

Altamimi, Z., Rebischung, P., Métivier, L., & Collilieux, X. (2016). ITRF2014: A new release of the international terrestrial reference frame modeling non-linear station motions: ITRF2014. *Journal of Geophysical Research: Solid Earth*, *121*(8), 6109–6131. https://doi.org/10.1002/2016JB013098

Artz, T., Halsig, S., Iddink, A., & Nothnagel, A. (2016). ivg::ASCOT: Development of a new VLBI software package [Software]. In *IVS 2016 General Meeting Proceedings "New Horizons with VGOS"*. https://ui.adsabs.harvard.edu/abs/2016ivs..conf..217A/abstract

Böhm, J., Urquhart, L., Steigenberger, P., Heinkelmann, R., Nafisi, V., & Schuh, H. (2013). A priori gradients in the analysis of space geodetic observations. In Z. Altamimi & X. Collilieux (Eds.), *Reference frames for applications in geosciences* (pp. 105–109). Springer Berlin Heidelberg. Retrieved from https://doi.org/10.1007/978-3-642-32998-2_17

Bolotin, S., Baver, K., Gipson, J., Gordon, D., & MacMillan, D. (2014). The VLBI data analysis softwareνSolve: Development progress and plans for the future [Software]. In D. Behrend, K. D. Baver, & K. Armstrong (Eds.), *IVS 2014 General Meeting Proceedings* (pp. 253–257). https://ui.adsabs.harvard.edu/abs/2014ivs..conf..253B/abstract

Datta-Barua, S., Walter, T., Pullen, S., Luo, M., Blanch, J., & Enge, P. (2002). *Using WAAS ionospheric data toEstimate LAAS short baseline gradients*. Standford University. Retrieved from https://web.stanford.edu/group/scpnt/gpslab/pubs/papers/DattaBarua/IONNTM/2002.pdf

Deller, A. T., Brisken, W. F., Phillips, C. J., Morgan, J., Alef, W., Cappallo, R., et al. (2011). DiFX-2: A more flexible, efficient, robust, and powerful software correlator [Software]. *Publications of the Astronomical Society of the Pacific*, *123*(901), 275–287. https://doi.org/10.1086/658907

Edwards, C. D. (1987). Short baseline phase delay interferometry. *TDA Progress Report 42-91*. Retrieved from https://ntrs.nasa.gov/api/citations/19880003301/downloads/19880003301.pdf

Garcia-Espada, S., González, R. B., & Grinde, G. (2023). Ny-Ålesund geodetic observatory. In K. L. Armstrong, D. Behrend, & K. D. Baver (Eds.), *International VLBI service for geodesy and astrometry 2021+2022 biennial report* (pp. 73–76). Retrieved from https://ivscc.gsfc.nasa.gov/publications/br2021+2022/nsnyal.pdf(NASA/TP-20230014975

Gipson, J. (2018). Sked VLBI scheduling software user manual [Software]. *Web document*. https://ivscc.gsfc.nasa.gov/IVS_AC/sked_cat/SkedManual_v2018October12.pdf

Gipson, J., Böhm, J., Bolotin, S., Gordon, D., Hobiger, T., Jacobs, C., et al. (2014). Final Report of IVS working group 4 (WG4) on data structures. In K. D. Baver, D. Behrend, & K. L. Armstrong (Eds.), *International VLBI service for geodesy and astrometry 2013 annual report*. Retrieved from https://ivscc.gsfc.nasa.gov/publications/ar2013/spcl-wg4.pdf(NASA/TP-2014-217522

Handirk, R., Varenius, E., Nilsson, T., & Garcia-Espada, S. (2026). Supporting data for publication: Obtaining local-tie vectors from short-baseline interferometry between legacy S/X and VGOS telescopes at Ny-Ålesund [Dataset]. *Zenodo*. https://doi.org/10.5281/zenodo.21412379

Handirk, R., Varenius, E., Nilsson, T., & Haas, R. (2023). Obtaining local-tie vectors from short-baseline interferometry. In K. L. Armstrong, D. Behrend, & K. D. Baver (Eds.), *International VLBI service for geodesy and astrometry general meeting 2022 proceedings*. Retrieved from https://ivscc.gsfc.nasa.gov/publications/gm2022/29/handirk/etal.pdf(NASA/CP-20220018789

IVS-AC. (2023). Gravitational deformation models for VLBI telescopes, version 2023-01-24. (Web document Retrieved from https://ivscc.gsfc.nasa.gov/IVS_AC/apriori/gravity_deform_model_v2023-01-24.txt, last access: 2024-02-22)

Kirkvik, A.-S., Dähnn, M., & Fausk, I. (2021). First results from the new station NYALE13S. In R. Haas (Ed.), *Proceedings of the 25th European VLBI Group for geodesy and astrometry working meeting* (pp. 115–119). Retrieved from https://www.oso.chalmers.se/evga/25/EVGA/2021/Cyberspace.pdf

Landskron, D., & Böhm, J. (2018). VMF3/GPT3: Refined discrete and empirical troposphere mapping functions. *Journal of Geodesy*, *92*(4), 349–360. https://doi.org/10.1007/s00190-017-1066-2

Malkin, Z. (2009). On comparison of the Earth orientation parameters obtained from different VLBI networks and observing programs. *Journal of Geodesy*, *83*(6), 547–556. https://doi.org/10.1007/s00190-008-0265-2

Martí-Vidal, I., Roy, A., Conway, J., & Zensus, A. J. (2016). Calibration of mixed-polarization interferometric observations. Tools for the reduction of interferometric data from elements with linear and circular polarization receivers. *Astronomy & Astrophysics*, *587*. https://doi.org/10.1051/0004-6361/201516063

McCallum, L., Chin Chuan, L., Krásná, H., McCallum, J., Böhm, J., McCarthy, T., et al. (2022). The Australian mixed-mode observing program. *Journal of Geodesy*, *96*(10), 67. https://doi.org/10.1007/s00190-022-01657-2

MIT/Haystack. (2020). Haystack observatory postprocessing system (HOPS) [Software]. Retrieved from https://www.haystack.mit.edu/haystack-observatory-postprocessing-system-hops/

Niell, A. E., Barrett, J. P., Cappallo, R. J., Corey, B. E., Elosegui, P., Mondal, D., et al. (2021). VLBI measurement of the vector baseline between geodetic antennas at kokee park geophysical observatory, Hawaii. *Journal of Geodesy*, *95*(6), 65. https://doi.org/10.1007/s00190-021-01505-9

Norwegian Polar Institute. (2025). Toposvalbard — Topographic map of Svalbard. Last access: 2025-06-03) Retrieved from https://toposvalbard.npolar.no/

Nothnagel, A. (2025). *Elements of geodetic and astrometric very long baseline interferometry*. TU Wien. https://doi.org/10.48436/jpxxh-74t10

Nothnagel, A., Artz, T., Behrend, D., & Malkin, Z. (2017). International VLBI service for geodesy and astrometry. *Journal of Geodesy*, *91*(7), 711–721. https://doi.org/10.1007/s00190-016-0950-5

Petrachenko, W., Niell, A., Corey, B., Behrend, D., Schuh, H., & Wresnik, J. (2012). VLBI2010: Next generation VLBI System for geodesy and astrometry. In U. M. S. Kenyon & M. C. Pacino (Eds.), *Geodesy for planet Earth, international Association of Geodesy Symposia* (Vol. 136, pp. 999–1006). Springer-Verlag Berlin Heidelberg. Retrieved from https://ivscc.gsfc.nasa.gov/technology/vgos-docs/VLBI2010_IAG2009_sub.pdf

Seitz, M., Bloßfeld, M., Glomsda, M., Angermann, D., Rudenko, S., Zeitlhöfler, J., & Seitz, F. (2026). DTRF2020: The ITRS 2020 realization of DGFI-TUM. *Journal of Geodesy*, *100*(2), 15. https://doi.org/10.1007/s00190-026-02032-1

Sovers, O. J., Fanselow, J. L., & Jacobs, C. S. (1998). Astrometry and geodesy with radio interferometry: Experiments, models, results. *Reviews of Modern Physics*, *70*(4), 1393–1454. https://doi.org/10.1103/revmodphys.70.1393

Tangen, O., Kierulf, H. P., Himle, S., & Garcia-Espada, S. (2024). Local ties and repeated stability measurements in Ny-Ålesund. In *Proceedings of the IVS 2024 General Meeting*.

Varenius, E., Haas, R., & Nilsson, T. (2021). Short-baseline interferometry local-tie experiments at the Onsala Space Observatory. *Journal of Geodesy*, *95*(5), 54. https://doi.org/10.1007/s00190-021-01509-5

VMF Data Server. (2026). VMF data server [Dataset]. https://doi.org/10.17616/R3RD2H

Xu, M. H., Savolainen, T., Bolotin, S., Bernhart, S., Plötz, C., Haas, R., et al. (2023). Baseline Vector repeatability at the sub-millimeter level enabled by radio interferometer phase delays of intra-site baselines. *Journal of Geophysical Research: Solid Earth*, *128*(3), e2022JB025198. https://doi.org/10.1029/2022jb025198